PHYSICSAccess Research Paper
ISSN Online: 2756-3898, ISSN Print: 2714-500X https://doi.org/10.47514/phyaccess.2024.4.2.010

First Principle Investigations of Structural, Electronic and Thermal Properties of Pristine, Metal and Non-Metal Doped Silicene for Thermoelectric Applications

Abdulkadir S Gidado[1], Reuben A Solomon[1], Lawal Abubakar[1], Fa'iza Ahmed[1] and Sulaiman R Haladu[1]

[1] Department of Physics, Bayero University Kano, Kano State, Nigeria

Corresponding E-mail: solomonreuben1010@gmail.com

Received 06-09-2024
Accepted for publication 18-10-2024
Published 21-10-2024

Abstract

Silicene, a two-dimensional hexagonal silicon layer, exhibits exceptional electronic and thermoelectric properties. However, its application in semiconductors is hindered by its zero-band gap, which could be overcome by modifying its electronic properties through doping. In this paper, Density Functional Theory (DFT) calculations were performed to investigate the band gap opening in silicene by studying the effect of magnesium and sulphur doping on its electronic, structural and thermal properties. Pristine silicene has a lattice constant of 3.86 Å and a zero-band gap. Upon doping with 12.5% S and Mg atoms, the lattice constant modifies to 3.45 Å and 3.93 Å, respectively, resulting in a direct band gap opening. For 25% Mg and S doping, the result shows that Mg and S effectively alter the band structure and the band gap of silicene monolayer at various configurations. The maximum band gap was 0.98 eV and 1.22 eV for Mg and S doping into the meta position to the reference point R, respectively. The power factor significantly increases with doping, reaching 1.20 x 10^{11} $WK^{-2}m^{-1}$ and 1.40 x 10^{11} $WK^{-2}m^{-1}$ for 12.5% Mg and S doping compared to 7.4 x 10^{10} $WK^{-2}m^{-1}$ for pristine silicene. This substantial enhancement indicates improved thermoelectric performance, making silicene a promising candidate for thermoelectric applications. Results demonstrate that tuning the band gap through doping can simultaneously enhance the power factor, highlighting the potential of Mg/S-doped silicene for efficient energy harvesting and conversion.

Keywords: DFT; Doping; Efficiency; Silicene; Thermal conversion.

I. INTRODUCTION

Two-dimensional materials, with their ultrathin structure and unique properties, have tended to spark tremendous interest in materials science [1]. These materials, such as graphene, transition metal dichalcogenides, and Silicene, have unique electronic, mechanical, optical and thermal characteristics, making them highly suitable materials for diverse applications in nanotechnology and beyond [2].

Like graphene, Silicene is a two-dimensional material and an analogue of graphene, consisting of six silicon atoms, has emerged as a subject of interest in the world of nanomaterials [3]. Due to its honeycomb lattice structure and intriguing electronic properties, this material has shown great potential

in nanoelectronics and optoelectronics, making it a focal point in research and technological exploration [4]. However, despite the unique properties of silicene, it is not a suitable material for some applications such as in electronics and thermoelectric devices, due to its zero-bandgap nature [5]. This disadvantage can be resolved by tuning silicene's properties via doping, which has further extended its potential for tailored applications. For instance, silicene, an allotrope of silicon and a counterpart to graphene exhibits excellent carrier mobility and thermal stability, making it suitable for various nano-electronic applications [6].

Amidst researchers, the contemporary issues over future energy consumption and the adverse effect of fossil fuels on the environment have initiated the effort to explore alternative energy sources. Consequently, this has necessitated the quest for new sources of energy other than fossil fuels [7]. Moreover, there is a critical need for energy conversion technologies as most of the energy produced is lost as heat in industrial environments and our daily lives, and conversion of these large amounts of the lost heat energy cannot be properly done and is inevitably wasted in the environment [8]. The invention of the thermoelectric effect presents a promising solution, enabling the direct conversion of heat to electricity or vice versa using thermoelectric materials [9]. Due to the ability of thermoelectric (TE) materials to directly convert heat into electricity, they have been attracting intensive attention and can play an important role in improving waste energy harvesting efficiency [10]. Thermoelectric materials that recover waste heat and transform it into electricity or vice versa can help resolve the current global energy crisis. Additionally, TE materials can reduce climate change resulting from global warming by creating opportunities for energy harvesting, smart sensors, and the new concept of automobiles, thermo power-wave sources, woodstoves, and diesel power plants [11]. Although the applications of thermoelectric materials like silicene are widened by enhancing their properties, it has mainly been used in small areas such as refrigerators, a cooling device for laser diodes, and cooling seats in automobiles due to their zero-bandgap and efficiency which is proportional to thermal properties such as power factor, Seebeck coefficient etc.

Efficient heat dissipation has been a significant problem usually faced by the semiconductor industry. For effective thermoelectric applications, materials with high power factor and low thermal conductivity materials are often preferred. Strategies such as doping, nanostructuring, and superlatticing have been employed in to suppress the thermal transport in the potential thermoelectric materials [12]. Understanding heat transport in doping is crucial to designing materials with suitable thermal transport properties. It's of great importance to understand how heat is transported in doping. Both electrons and phonons contribute to heat transfer in solids. Doping has emerged as a potent strategy for manipulating the band gap of two-dimensional material and silicene, possessing intrinsic optical and thermoelectric attributes, can experience enhanced properties through doping interventions [13]. Elemental doping has been used to tune the band gap of 2D materials through elemental doping using density functional theory. However, recent studies have effectively engineered the band gap of 2D materials through elemental doping using the density functional theory. The structural, electronic and vibrational properties of silicene were studied via the first principle calculations. These calculations revealed that silicene exhibits a buckled honeycomb structure with a direct band gap [14]. Also, the first principle study was employed to investigate the stability and electronic properties of silicene, it was found that silicene is dynamically stable and exhibits a tunable band gap, making it a promising material for electronic applications [15].

Silicene, a 2D material, exhibits a zero-bandgap nature, limiting its applications in the semiconductor industry. To overcome this limitation, substitutional doping of silicene monolayer sheets with metal and non-metal atoms has been explored. Building upon existing research [5, 16, 17], this paper, investigates the effects of Magnesium (Mg) and Sulphur (S) on silicene's band structure, Seebeck coefficient, and power factor, with a focus on phonon transport. However, previous studies have overlooked the critical aspect of vacancy transformation due to dangling bond saturation during doping which will be considered in this work. This investigation will not only contribute to a deeper understanding of doped silicene but also hold the promise of designing tailored silicene-based materials for specific functionalities in advanced technological applications.

II. Theoretical Background

Density-functional theory (DFT) is a computational quantum mechanical modelling method usually employed by physicists, chemists and materials scientists to explore the electronic structure or nuclear structure, specifically at the ground state of many-body systems, in particular atoms, molecules, and the condensed phases. With this theory, the properties of a many-electron system can be studied using functional, that is function of another function. In the case of DFT, these are functionals of the spatially dependent electron density.

Usually, in many-body electronic structure calculations, the nuclei of the molecules or clusters in question are assumed to be fixed (the Born–Oppenheimer approximation), generating a static external potential V, in which the electrons are moving. A stationary electronic state is then described using a wavefunction $\Psi(r_1, \ldots, r_N)$ conforming to the many-electron time-independent Schrödinger equation.

$$\hat{H}\Psi = \left[\hat{T} + \hat{U} + \hat{\nabla}\right]\Psi = \left[\sum_{i=1}^{N}\left(\frac{-\hbar}{2m_i}\nabla_i^{\,2}\right) + \sum_{i=1}^{N} V(r_i) + \sum_{i=1}^{N} U(r_i, r_i)\right]\Psi = E\Psi \quad (1)$$

Where, for the N-electron system, Ĥ is the Hamiltonian, E is the total energy, $\hat{T}$ is the kinetic energy, $\hat{V}$ is the potential energy from the external field due to positively charged nuclei,

and Û is the electron-electron interaction energy. The operators $\hat{V}$ and $\hat{U}$ are called universal operators, as they are the same for any N-electron system, while $\hat{V}$ is system-dependent. This complicated many-particle equation is seen not to be separable into simpler single-particle equations as it contains the interaction term $\hat{U}$.

DFT provides an appealing, more versatile alternative because it provides a way to systematically map the many-body problem, with Û, onto a single-body problem without Û. In DFT the key variable is the electron density n(r), which for a normalized Ψ is given by (2).

$$n(r) = N \int d^3 r_N \, \Psi^0\left(r, r_{2,} \ldots, r_N\right)\Psi\left(r, r_{2,} \ldots, r_N\right) \quad (2)$$

Equation 2 is reversible, if the ground-state density is known, moreover, to calculate the equivalent ground-state wave function, we know that Ψ is a unique functional of n_0, [16],

$$\Psi_0 = \Psi[n_0] \quad (3)$$

Consequently, the ground-state expectation value of an observable $\hat{O}$ is also a functional of:

$$O[n_0] = \langle \Psi[n_0] | \hat{O} \, | \Psi[n_0] \rangle \quad (4)$$

In particular, the ground-state energy is a functional of n_0.

$$E_0 = E[n_0] = \langle \Psi[n_0] | \hat{T} + \hat{U} + \hat{\nabla} | \Psi[n_0] \rangle \quad (5)$$

The contribution due to the external potential $\langle \Psi[n_0] | \hat{V} | \Psi[n_0] \rangle$ can be expressed in terms of the ground-state density as n_0.

$$V[n_0] = \int V(r) n_0(r) d^3 r \quad (6)$$

In a more generalised way, the contribution due to the external potential $\langle \Psi | \hat{V} | \Psi \rangle$ can be expressed explicitly as a function of the density n as follows:

$$V[n] = \int V(r) n(r) d^3 r \quad (7)$$

$T[n]$ and $U[n]$ are called universal functionals, while $V[n]$ is called a non-universal functional, as it depends on the system under study. Having specified a system, i.e., having specified V, one then has to minimize the functional.

$$E[n] = T[n] + U[n] + \int V(r) n(r) d^3 r \quad (8)$$

Concerning $n(r)$, assuming one has reliable expressions for $T[n]$ and $U[n]$. A successful minimization of the energy functional will yield the ground-state density n_0 and thus all other ground-state observables.

The variational problems of minimizing the energy functional can be solved using the Lagrangian method of undetermined multipliers [16]. First, one has to consider an energy functional that does not explicitly have an electron-electron interaction energy term,

$$E_s[n] = \langle \Psi_s[n] | \hat{T}_s + \hat{V}_s | \Psi_s[n] \rangle \quad (9)$$

Where $\hat{T}_s$ denotes the kinetic-energy operator, and $\hat{V}_s$ is the effective potential with which the particles move. Consequently, we solve the so-called Kohn–Sham E_s equations of this auxiliary non-interacting system,

$$\left[\frac{-\hbar^2}{2m}\nabla^2 + V_s(r)\right]\varphi_i(r) = \varepsilon_i \varphi_i(r) \quad (10)$$

which yields the orbitals φ_i that reproduces the density $n(r)$ of the original many-body system

$$n(r) = \sum_{i=0}^{N} |\varphi_i(r)|^2 \quad (11)$$

However, the formation energy of a system can be determined using

$$E_f = E_t - N_{si}\mu_{si} - \sum_i N_i \mu_i \quad (12)$$

Where E_t is the total energy of the doped system, μ_{si} and N_{si} are the chemical potential and total number of Si atoms respectively, and N_i and μ_i are the total number and chemical potential of the dopant atom(s) [16].

III. COMPUTATIONAL METHOD

All calculations were carried out within the density functional theory framework (DFT) [8], as implemented in the Quantum ESPRESSO code [17]. The Generalized gradient approximation (GGA) with the Perdew-Burke –Enzehof (GGA-PBE) exchange functional method was employed to obtain the electronic, structural calculations [18]. For the electronic wave function description, the projected augmented wave (PAW) method was used. To minimize errors, a self-consistent convergence was achieved for all calculations [16]. The optimized plane wave cut-off energy was obtained at 45Ry, while the Mokhorst-Pack scheme K-point sampling of the Brillouin zone was achieved at 15 x 15 x 1. The plane wave energy cut-off and k-point convergence are demonstrated in Fig. 1(a) and (b).

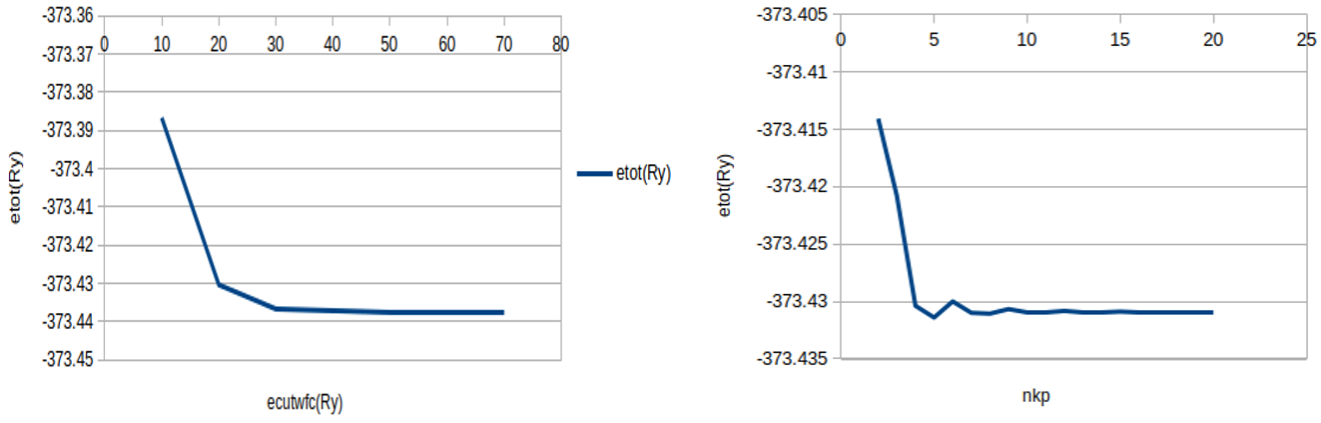

(a) (b)

Fig. 1. Wave function optimization (b) K-points optimization.

Since silicene comprises of 8 atoms of silicon arranged in a hexagonal structure, each silicon atom contributes 12.5% of its effect to the silicene monolayer. To alter the electronic configuration of silicene, we substituted each silicon atom with magnesium (Mg) and sulphur (S) at two percentages 12.5% (1 atom of Mg/S) and 25% (2 atoms of Mg/S) respectively. For 25% doped systems we designated the initial substitution site of 12.5% Mg or S doped as the reference point. The second substitution was then made at Ortho, Meta and Para positions relative to the reference point R, resulting in three distinct configurations. These configurations were identified as M_1, M_2, and M_3 for the 25% Mg-doped system and S_1, S_2, and S_3 for the 25% S-doped system. The structural model of pristine and doped monolayer silicene was viewed using XcRYSDEN software.

IV. Result and Discussion

A. *Optimized Structure of Silicene*

Our investigation into the structural, electronic, and thermoelectric properties of a 2x2x1 supercell of silicene reveals several key features. The optimized lattice constant of 3.86 Å and Si-Si distance of 2.27 Å are in good agreement with previously reported values of 3.89 Å for lattice constant and 2.22 Å bond length [5, 21].

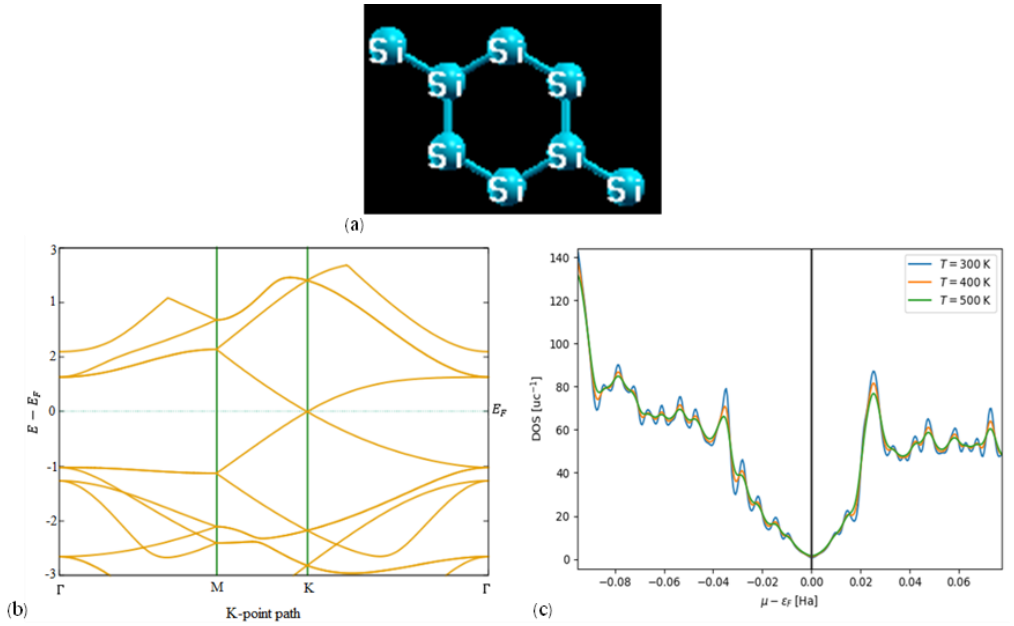

Fig. 2. Optimized structure Band structure, (b) Band structure and (c) DOS of pure silicene.

B. *Optimized and Electronic Properties of Silicene, Silicene-Doped Magnesium and Silicene-Doped Sulfur*

The band structure is a graphical representation of the energy levels of electrons in solids, providing valuable information about the electronic properties of the material. Key properties such as band-gap energy, electron mobility, conductivity, and valence and conduction energies can be deduced from the band structure, which is crucial for designing and optimizing electronic devices.

Fig. 2(a) and 2(b) depict the optimized and electronic band structure of silicene, showing a zero band gap, indicating that silicene is a semi-metal, consistent with earlier report [21]. The DOS plot confirms this, with a zero value at the Fermi energy as seen in Fig 2(c).

Fig. 3(b) and 4(b) show the optimized band structure of 12.5% silicene doped with Mg and S, respectively, with significantly altered structural and electronic properties. The lattice constant was found to increase to 3.93 Å for Mg doping and decrease to 3.45 Å for S doping, indicating lattice expansion and contraction, respectively. The Si-Si and dopant-Si distances also change to 2.31 Å for Mg and 2.23 Å for the S-doped system, reflecting the different atomic radii of Mg and S.

The electro-negativity of the dopant atoms also plays a crucial role, with Mg (1.31) being less electronegative than Si (1.90) and S (2.58) being more electronegative. This leads to a change in the bonding characteristics.

To obtain the stability of the doped system we calculated the formation energy E_f using (12). The formation energy of the S-doped system is negative (-0.659 eV), indicating that it is energetically favourable, compared to the positive formation energy of the Mg-doped system (1.89 eV), compared. The Mg-doped system shows a p-type behaviour with an excess of electrons, while the S-doped system exhibits n-type behaviour with a deficiency of electrons.

Fig. 3(c) and 4(c), the DOS plots of Mg and S-doped systems respectively, reveal a zero value around 0.2Ha and -0.2Ha for the Mg-doped and S-doped systems, respectively, indicating the presence of impurity states. The band gap values of 0.51 eV and 0.643 eV were obtained for the Mg-doped and

S-doped systems, respectively. This change in the band structure can be attributed to the symmetry breaking of silicene structure due to Mg or S- doping, suggesting that Mg/S doping can effectively tune the electronic properties of silicene.

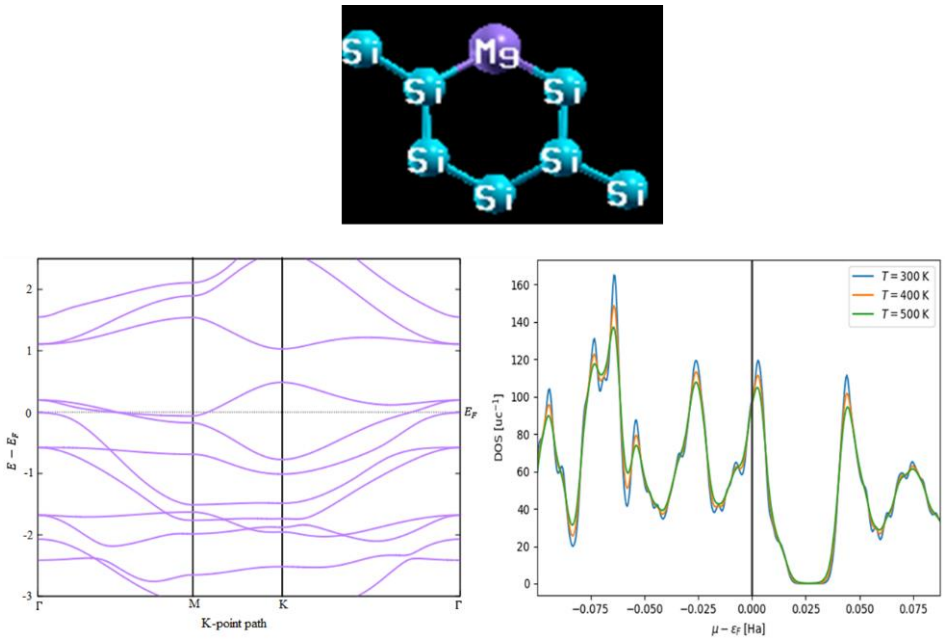

Fig. 3. (a) Optimized structure (b) Band structure and (c) DOS of 12.5% Mg-doped silicene.

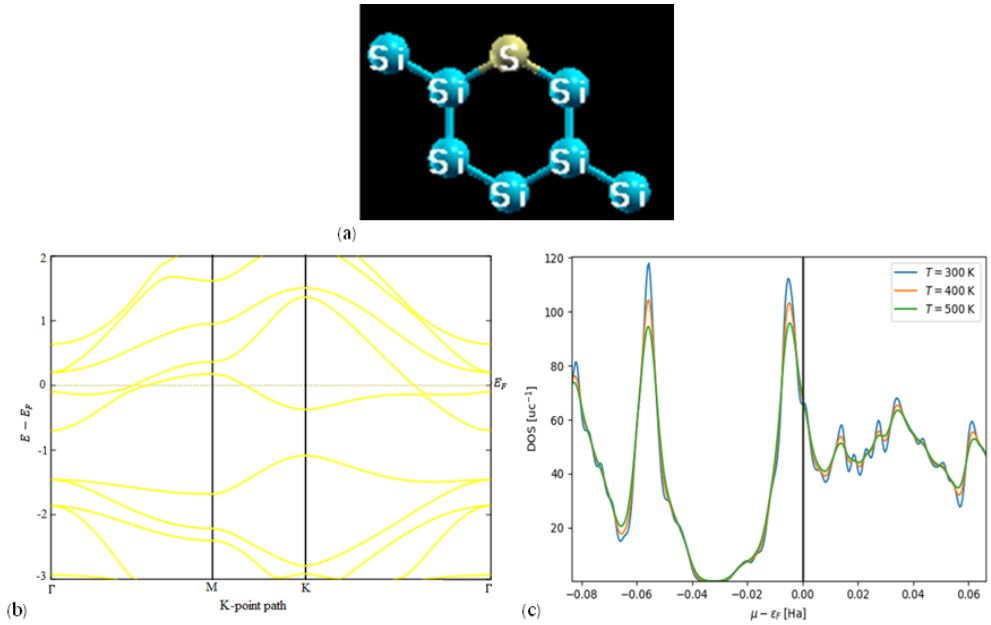

Fig. 4. Optimized structure Band structure, (b) Band structure and (c) DOS of 12.5% S- doped silicene.

Fig. 5, 6 and 7 represent the optimized structure of M_1, M_2 and M_3 respectively. The M_1 band gap was found to be 0.004 eV, 0.98 eV for M_2 and 0 eV for M_3. The band gap of M_3 and M_1 were lower than that of the mono-doped Mg system, while that of M_2 is higher, indicating a linear relationship between concentration ratio and band gap [19]. Our result for the dual Mg-doped system reveals that atomic positioning is crucial in determining the bandgap and the concentration ratio.

The formation energy of silicene with mono-doped silicene is less than that of the dual-doped system showing that the mono-doped silicene system is more energetically favourable compared to the dual-doped system. Our DFT calculations show that the Mg dual doped system can be arranged in decreasing order of formation energy as M_1 (2.94 eV) < M_3 (3.11 eV) < M_2 (3.45 eV) which is in the same sequence with Ga doped Silicene as in [5]. Since the lower the formation

energy, the higher the energetic stable of the structure, thus, M_1 is the most stable energetic structure.

Fig. 8, 9 and 10 depict the optimized S_1, S_2 and S_3 structures respectively. The band gaps were found to be 0.00114 eV for S_1, 1.20 eV for S_2 and 0 eV for S_3. The band gaps of S_3 and S_1 are lower than that of the monodoped S system, while that of S_2 was found to be higher. This sequence is the same as that of the Mg-doped system, except that the Fermi energy crosses the conduction band in S-doped systems.

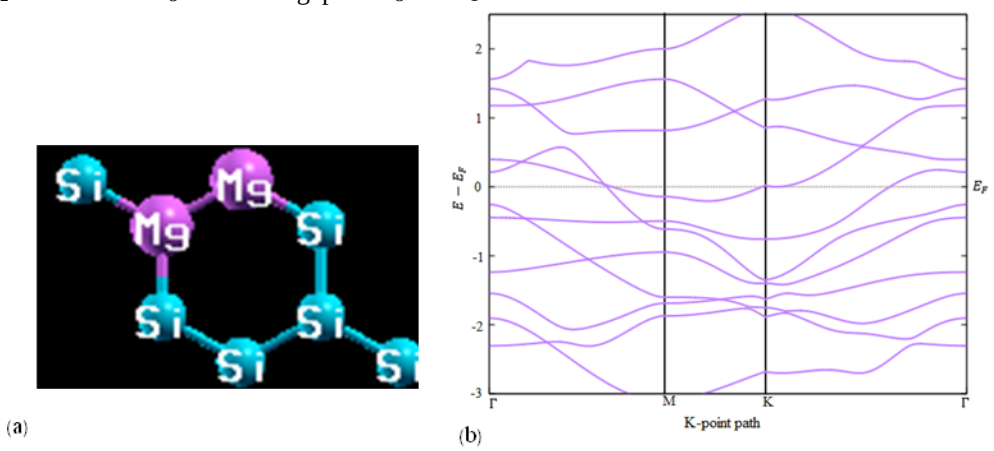

Fig. 5. (a) Optimized structure and (b) Band structure of M_1.

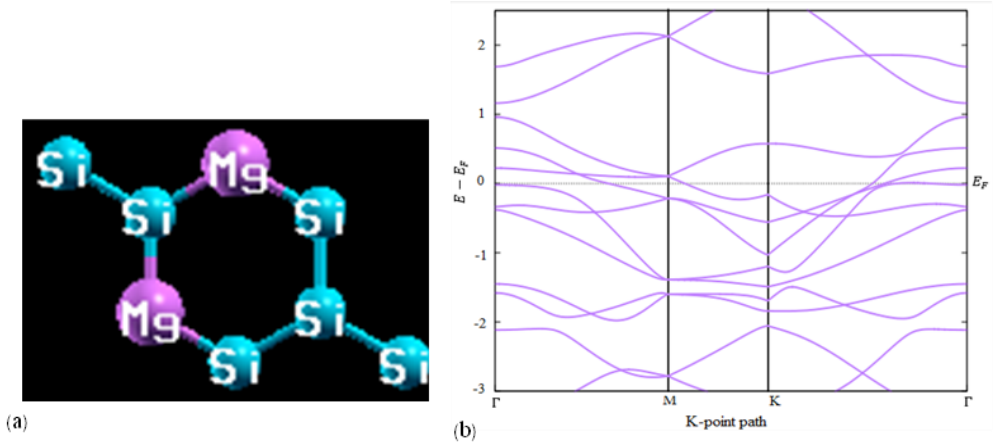

Fig. 6. (a) Optimized structure and (b) Band Structure of M_2.

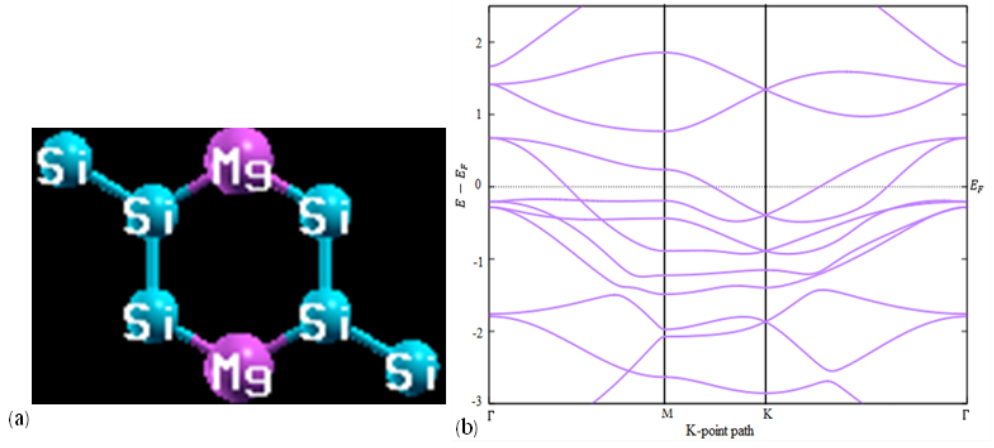

Fig. 7. (a) Optimized structure and (b) Band Structure of M_3.

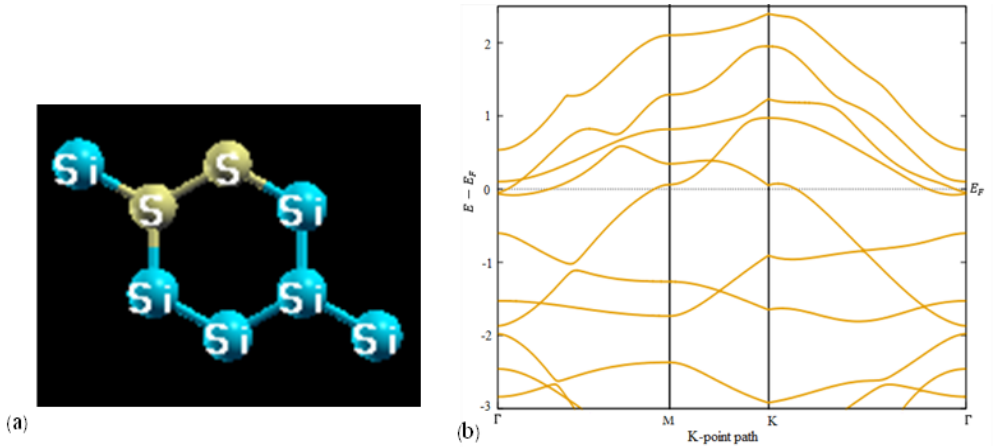

Fig. 8. (a) Optimized structure and (b) Band Structure of S_1.

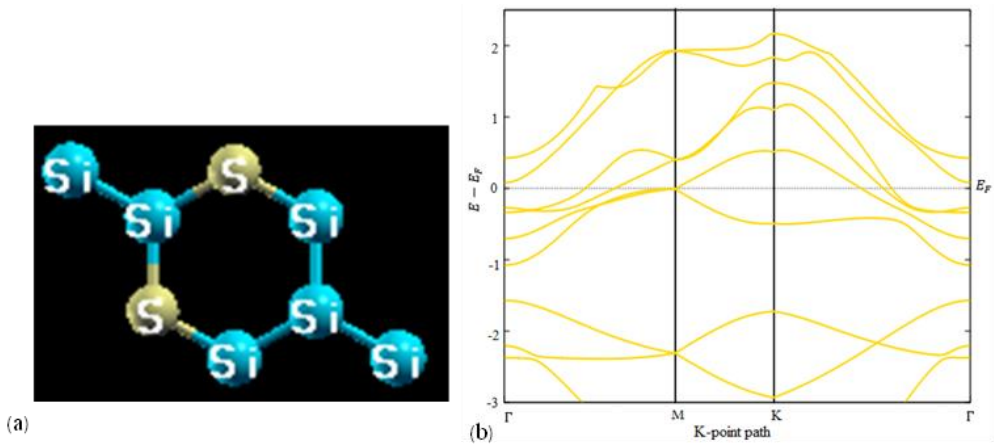

Fig. 9. (a) Optimized structure and (b) Band Structure of S_2.

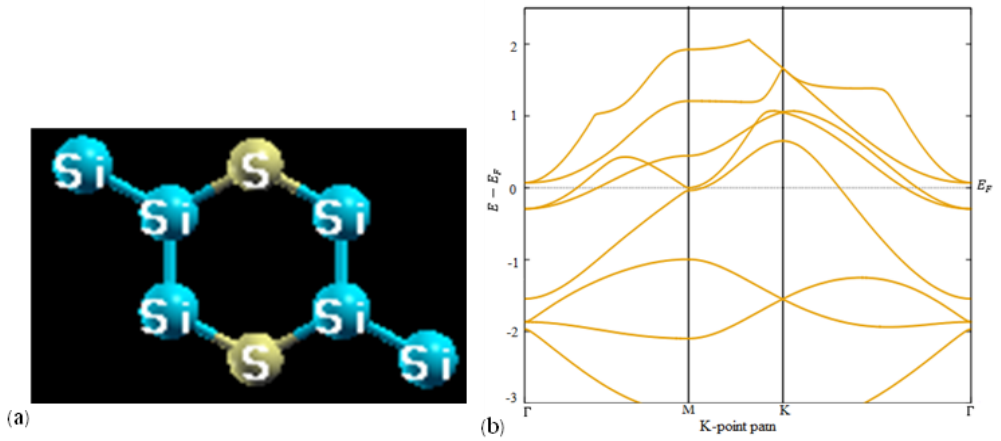

Fig. 10. (a) Optimized structure and (b) Band Structure of S_3.

C. Thermoelectric Properties of Silicene, Silicene-Doped Magnesium and Silicene-Doped sulfur

Doping with magnesium and sulfur also modifies the thermoelectric properties of native silicene, as changes in the electronic properties of native silicene occur. To investigate this effect, we calculate the thermoelectric properties of native silicene and compare them to those of silicene doped with magnesium and sulfur respectively. The power factor for pure silicene and its doped variants was computed via Boltztrap2 code, using (13) [20].

$$PF = S^2 \times \sigma \quad (13)$$

Where S is the Seebeck coefficient and σ is the electrical conductivity of the system.

The power factor of pristine silicene versus chemical potential is presented in Fig. 11(a) for three different values of temperature, 300 K (blue), 500 K (red) and 600 K (green). The power factor increases with temperature due to the direct relation between the Seebeck coefficient and temperature, which determines the factor power factor (that is S~T). The power factor was found to be $\sim 7 \times 10^{10}\ WK^{-2}m^{-1}$ for 600 K around the Fermi energy. The zero value of the power factor at the Fermi energy is due to the zero value of the Seebeck coefficient at this point.

Fig 11(b) and (c) show the power factor of 12.5% Mg- and S- atom doped silicene, respectively. The crossing of the valence bands in Mg- and conduction bands in S-doped silicene increases its power factor to $\sim 1.2 \times 10^{11}\ WK^{-2}m^{-1}$ and 1.40 x 10^{11} $WK^{-2}m^{-1}$ respectively. This enhancement was due to the increase in the Seebeck coefficient in both systems.

The power factor of M_1, M_2 and M_3 are $\sim 1.08 \times 10^{11}\ WK^{-2}m^{-1}$, $1.31 \times 10^{11}\ WK^{-2}m^{-1}$ and $1.19 \times 10^{11}\ WK^{-2}m^{-1}$ respectively. As a result, the power factor of M_1 is lower compared to Mg mono-doped silicene due to the repulsive interaction between Mg atoms, leading to an increased electronic conductivity and decreased Seebeck coefficients.

We note that the same scenario occurs for S-doped silicene with two S-atoms as in the Mg-doped silicene with two Mg atoms, so we do not present the result for the S-silicene system with two S-atoms.

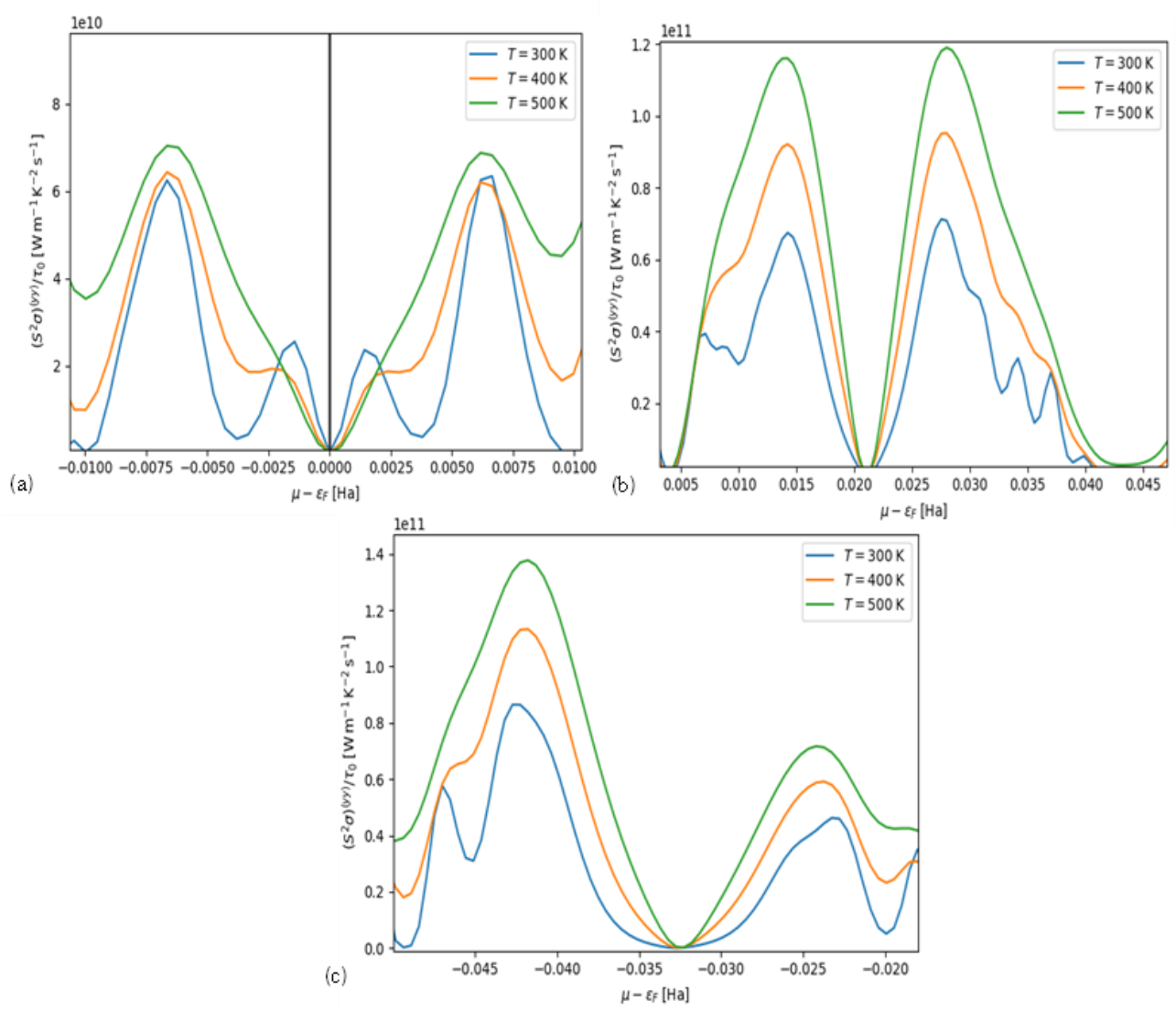

Fig. 11. (a) The power factor of pure silicene (b) Mg- and (c) S- 12.5% doped silicene.

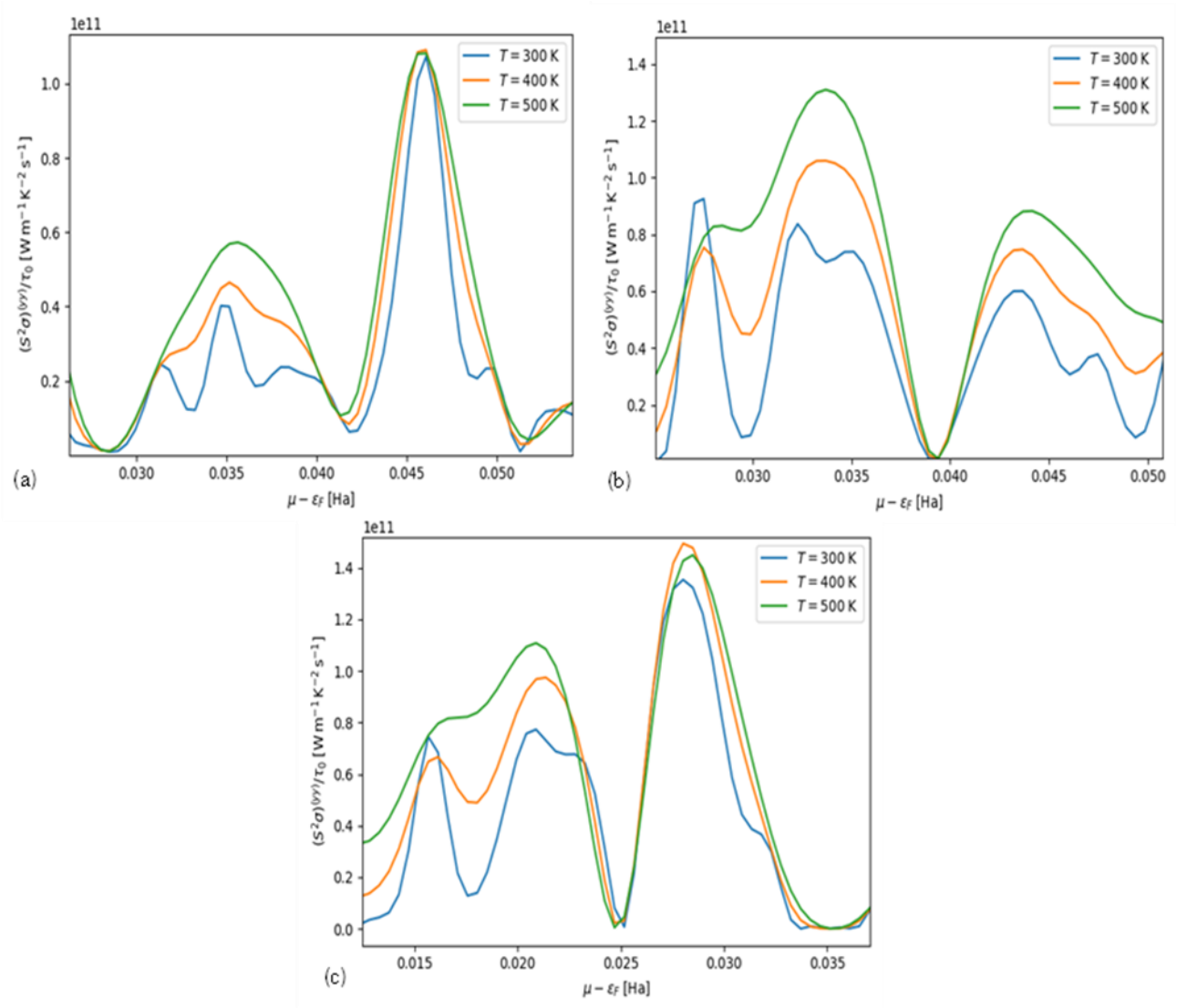

Fig. 12. The power factor of (a) M_1 (b) M_2 and (c) M_3.

V. Conclusion

In conclusion, we employed the density functional theory (DFT) to investigate the effects of configuration, and interatomic distance on structural, electronic and thermoelectric properties of 2x2x1 monolayer pure silicene, silicene doped with magnesium and silicene doped with sulphur. Despite silicene's favourable properties, its zero-band gap hampers its ability to effectively transit between conductive and non-conductive states, limiting its application in devices requiring a large OFF/ON ratio and leading to low power factors and thermal efficiency. Results obtained show that doping Mg/S into the silicene monolayer opens up its band gap, making it a semiconductor. The configuration and the dopant concentration ratio control the band gap, according to our calculations. For 12.5% Mg- and S- doped silicene the band gap was found to be 0.51 eV and 0.643 eV, while the power factor increased by approximately 1.6 and 1.9 times that of pure silicene. For the co-doping systems despite the increased concentration to 25%, only the M_2 or S_2 showed higher band gaps and thermoelectric properties than their respective mono-doped counterparts. This research suggests that the best configuration for either metal/metal or non-metal/non-metal dopant in a hexagonal structured system is the R-meta. Our results demonstrate that tuning the band gap through doping can simultaneously enhance the power factor, making silicene a promising candidate for thermoelectric applications.

Reference

[1] S. K. Novoselov, A. K. Geim, V. S. Morozov, D. Jiang, Y. Zhang, V. S. Dubonos, V. Grigorieva and A. Firsov, "Electric field effect in atomically thin carbon films," Science, vol. 308, no. 5696, pp. 666-669, 2004.

[2] S. Z. Butler, S. M. Hollen, L. Cao, Y. Cui, J. A. Gupta, H. R. Gutiérrez, T. F. Heinz, S. S. Hong, J.

Huang, A. F. Ismach, E. Johnston-Halperin, M. Kuno, V. V. Plashnitsa, R. D. Robinson, R. S. Ruoff, S. Salahuddin, J. Shan, L. Shi, M. G. Spencer, M. Terrones, W. Windl, and J. E. Goldberger, "Progress, Challenges, and opportunities in two-dimensional materials beyond graphene," ACS Nano, vol. 7, no. 4, pp. 2898-2926, 2013.

[3] P. Vogt, P. De Padova, C. Quaresima, J. Avila and E. Frantzeskakis, "Siicene: Compelling experimental evidence for graphene-like two-dimensional silicon," Phy. Rev. Lett., pp. 1-12, 2012.

[4] Y. Tao, C. Mingji, C. Hao-sen and Y. Pei, "Strain rate effect on the out-of-plane dynamic compressive behaviour of metallic honeycombs: Experiment and theory," Comp. Struct., vol. 132, no. 11, pp. 644-651, 2015.

[5] N. R. Abdullah, J. A. Botan and G. & Vidar, "DFT study of tunable electronic, magnetic, thermal and optical properties of a Ga2Si6 monolayer," Solid State Science, vol. 2, no. 3, pp. 1-9, 2022.

[6] S. Cahangirov, M. Topsakal, E. Akturk, H. Sahin and S. Ciraci, "Two- and one-dimensional honeycomb structures of silicon and germanium," Physical Review Letters, vol. 14, no. 5, pp. 33-36, 2009.

[7] S. Sharma and K. P. Sudhir, "A first principle study of electronic band structures and effective mass tensors of thermoelectric materials: PbTe, Mg2Si, FeGa3, and CoSb3.," Computational Materials Science, vol. 85, pp. 340-346, 2015.

[8] J. J. M. Gutierrez, C. Jinga, F. Marco and M. N. A. Hussein, "A review of recent progress in thermoelectric materials through computational methods," Materials for Renewable and Sustainable Energy, vol. 9, no. 3, pp. 16-23, 2020.

[9] Y. Z. Zhang, Y. H. Han and Q. S. Meng, "The performance of Mg2Si-based thermoelectric material prepared from Mg2H2," Material Research Institution, vol. 19, no. S1, pp. S1-264-S1-268, 2015.

[10] H. Alam and S. Ramakrishna, "A review on the enhancement of figure of merit from bulk to nano-thermoelectric material," Nano Energy, vol. 2, no. 2, pp. 190-212, 2013.

[11] X. Liu, J. Ruchita, O. Esther, J. Conrad, C. Piotr, Q. Ming and N. Brian, "State of the heart composition, fabrication, characterisation, and modelling methods cement-based thermoelectric materials for low-temperature applications.," Renewable and Sustainable Energy Reviews, 2020.

[12] M. Dresselhaus, G. S. Chen, M. Y. Tang, R. Yang, H. Lee, D. Wang, Z. Ren, -P. Fleurial J and P. Gogna, "New Directions for Low-Dimensional Thermoelectric Materials," Advance Materials, vol. 19, pp. 1043-1053, 2017.

[13] N. R. Abdullah, T. K. Mohammad, O. R. Huar, M. Andrei and G. Vidar, "Spin-polarised DFT modelling of electronic, magnetic, thermal and optical properties of silicene doped transition metals," Low-Dimensional System & Nanostructures, pp. 1-9, 2021.

[14] N. D. Drummond, V. Zolyomi and V. I. Fal'ko, "First Principle Study of Silicene: Structural, Electronic and Vibrational Properties," J. of Phy.; Cond. Matt., vol. 6, no. 111, pp. 075423-1-075423-7, 2012.

[15] R. Wang, G. Wang and X. Zhao, "First-Principle Investigation of the Stability and Electronic Properties of Silicene," Journal of Physics: Condensed Matter, vol. 22, no. 27, 2015.

[16] P. Hohenberg and W. Kohn, "Inhomogeneous electron gas," Physical Review, vol. 136, no. 3B, pp. B864-B871, 1964, doi: 10.1103/PhysRev.136.B864.

[17] P. Rani and V. K. Jindal, "Designing band gap of graphene by B and N dopant atoms," Royal Society of Chemistry Advances, vol. 3, pp. 802-812, 2013.

[18] W. Kohn and L. J. Sham, "Self-consistent equations including exchange and correlation effect," Physics Letters A, vol. 21, no. 140, pp. 1133-1138, 1965.

[19] P. Giannozzi, S. Baroni, N. Bonini, M. Calandra, R. Car, C. Cavazzoni and N. Marzari, "Quantum ESPRESSO: a modular and open-source software project for quantum simulations of materials.," Journal of Physics: Condensed Matter, 21(39), 395502., vol. 21, no. 39, pp. 395502-395520, (2009).

[20] J. P. Perdew, K. Burkey and M. Ernzerhof, "Generalized gradient approximation," Review letters, vol. 77, no. 18, pp. 3865-10, 1996.

[21] A. P. Mauludi and M. Wafa, "Electronic structures of silicene Doped with Galium: First Principle study," Edition Diffusion Presse Sciences, vol. 2015, no. 03003, pp. 1-3, 2015.